Contents lists available at Science-Gate

International Journal of Advanced and Applied Sciences

Journal homepage: http://www.science-gate.com/IJAAS.html

Effect of SiO_2 on the foamability, thermal stability and interfacial tension of a novel nano-fluid hybrid surfactant

Mohammed Falalu Hamza [1, 2], Chandra Mohan Sinnathambi [1, 2], Zulkifli Merican Aljunid Merican [1, 2], Hassan Soleimani [1, 2, *], Karl D. Stephen [2, 3]

[1]*Fundamental and Applied Science Department, UTP, 32610 Bandar Seri Iskandar, Perak Darul Ridzuan, Malaysia*
[2]*Center of Research in Enhanced Oil Recovery, UTP, 32610 Bandar Seri Iskandar, Perak Darul Ridzuan, Malaysia*
[3]*Petroleum Engineering Department, UTP, 32610 Bandar Seri Iskandar, Perak Darul Ridzuan, Malaysia*

ARTICLE INFO

Article history:
Received 10 August 2017
Received in revised form
27 October 2017
Accepted 18 November 2017

Keywords:
Enhanced oil recovery
FAWAG
Composite material
Hybrid
Nanoparticles

ABSTRACT

In foam assisted water alternating gas (FAWAG) method, thermal stability, foamability and interfacial effect of foaming agents (surfactants) are important properties governing the success of oil recovery. The effect of high reservoir temperature is detrimental to these properties, which becomes a great challenge for the applications of surfactants in enhanced oil recovery (EOR). Silica nano-fluid (SiO2), which is a recently employed technology, has been utilized to improve the rheology, stability and interfacial properties of surfactants. This study is aimed at investigating the effect of SiO_2 in improving the thermal stability, relative foamability and interfacial (IFT) effect of industrial based surfactant (IBS). Design Expert Software (DOE) using central composite design (CCD) at five levels (-1.68 to +1.68) was employed in the experimental design. The chemical interaction between the SiO_2 and IBS in the novel nano-fluid hybrid surfactant (SiO_2-IBS) had been successfully established using different spectroscopic instruments (FTIR, XRD, FESEM etc.). Furthermore, under the optimum conditions established, SiO_2 had significant effects on the relative foamability and thermal stability of the hybrid material (SiO_2-IBS) at 25-110 ^oC, and their synergistic effect had been quantified in the multivariate models (cubic). However, the IFT result indicated that presence of the SiO_2 in the hybrid had reduced the IFT drastically from 120.3 ± 9.8 mN/m to 10.6 ± 6.8 mN/m. Consequently, the novel SiO_2-IBS nano hybrid surfactant could be a suitable flooding agent in the high temperature reservoirs for application in FAWAG method.

1. Introduction

Enhanced Oil Recovery (EOR), an advanced technology employed in oil industry, has the potential to extract residual oil after primary and secondary technologies (Ahmadi et al., 2015; Hamza et al., 2017). The advantage of EOR over the conventional technologies (primary and secondary) involves the injection of foreign fluids (surfactants, polymers, gases etc.) or energy capable of interfering with oil/water/rock systems to mobilize the oil to the surface (Alagorni et al., 2015). Approximately, 40 to 60 % of oil production rate has been attained with the utilization of the EOR technologies (Muggeridge et al., 2014). Water Alternating Gas (WAG) technology, which requires simultaneous injection of gas and water into the reservoir has been the most frequently employed EOR technology (Riazi and Golkari, 2016). However, early gas breakthrough, gravity override and viscous fingering constituted the main challenge in the WAG execution, and result to poor sweep efficiency over time (Qureshi et al., 2016). Efforts to overcome these problems had led to the development of foams to assist in WAG, and this technology is referred to as Form Assisted Water Alternating Gas (FAWAG). In FAWAG, the gas is injected into surfactant solution, which is then trapped to form foam bubbles, these help to control the gas mobility and improve oil recovery (Shabib-asl et al., 2014, Tunio and Chandio, 2012). Despite high oil recovery achieved in FAWAG, obtaining stable foams in high temperature oil reservoirs are difficult and consequently affect their overall performance (Kapetas et al., 2016). However, silica nanofluid (SiO2), which is a recently employed technology, has been found to show a remarkable

* Corresponding Author.
Email Address: hassan.soleimani@utp.edu.my (H. Soleimani)
https://doi.org/10.21833/ijaas.2018.01.015

improve on the rheology, stability and interfacial properties of surfactants (Esmaeeli Azadgoleh et al., 2014; Sharma et al., 2016). The effects of SiO2 on stabilizing foams in different type of surfactants have been reported (Xue et al., 2016; Sun et al., 2015). In this study, SiO2 and industrial based surfactant (IBS) were used to formulate a new nanofluid hybrid surfactant (SiO2-IBS), and the effect of the SiO2 on the foamability, thermal stability and interfacial tension of SiO2-IBS had been investigated. The Design Expert Software (DOE) has been used to develop experimental combinations with respect to the concentrations of SiO2 and IBS, as well as aging. The central composite design (CCD) and response surface methodology (RSM) were applied for optimization and modeling.

2. Materials and methods

The SiO_2 was purchased as a bare nano powder (20-30 nm, 99.5 wt %, amorphous) from US Research nanomaterials, Inc. USA. It has the surface area of 180-600 m2/g, bulk density and true density of < 0.10 and 2.4 g/cm^3, respectively. While the surfactant (IBS), was supplied from a Malaysian local oil company. The compositions of synthetic brine (3.5 %) used is presented in Table 1.

Table 1: Synthetic brine composition

S/N	Salt name	Chemical formula
1	Sodium chloride	NaCl
2	Potassium chloride	KCl
3	Magnesium chloride hexahydrate	$MgCl_2.6H_2O$
4	Calcium chloride dihydrate	$CaCl_2.2H_2O$
5	Sodium bicarbonate	$NaHCO_3$
6	Sodium sulfate	Na_2SO_4
7	Strontium chloride	$SrCl_2.6H_2O$

2.1. Development of combinations

The DOE software was employed to statistically design the formulation combinations using a CCD. Table 2 shows the range values of SiO_2, IBS and aging chosen at five levels from -1.68 to +168. The choice of this range was because of the conflicting levels of optimum conditions for SiO_2, IBS and aging from the literature.

Table 2: Processed factors of independent variables at five levels intervals

Independent variables	Process level of variables at five levels intervals (-α to +α)				
SiO_2 (%) IBS (%) Aging (days)	-1.68	-1	0	+1	+1.68

The actual processed factors of all the input variables were keyed into the software and Table 3 was generated. The table described 17 different formulation combinations with 6 central points (formulations 15-20) as replicates to minimize error according to CCD. These had let to the development of 20 experimental combinations formulated.

Table 3: Experimental combinations of input variables (in terms of processed factors)

S/N	Standard Experiments	Processed level of variables Factor A IBS	Factor B SiO_2	Factor C Aging
1	S11	0.00	-1.68	0.00
2	S4	1.00	1.00	-1.00
3	S7	-1.00	1.00	1.00
4	S2	1.00	-1.00	-1.00
5	S8	1.00	1.00	1.00
6	S16	0.00	0.00	0.00
7	S15	0.00	0.00	0.00
8	S9	-1.68	0.00	0.00
9	S5	-1.00	-1.00	1.00
10	S13	0.00	0.00	-1.68
11	S6	1.00	-1.00	1.00
12	S17	0.00	0.00	0.00
13	S1	-1.00	-1.00	-1.00
14	S18	0.00	0.00	0.00
15	S3	-1.00	1.00	-1.00
16	S20	0.00	0.00	0.00
17	S19	0.00	0.00	0.00
18	S14	0.00	0.00	1.68
19	S12	0.00	1.68	0.00
20	S10	1.68	0.00	0.00

2.2. Chemical formulations

In EOR process, the low concentrations of injecting chemicals are important to achieve high recovery factor at low costs to maximize profit (Han et al., 2013). In this study, the concentrations of the SiO_2 and IBS in brine are in the range of -1.68 to +1.68 according to Table 2. These solutions were then combined to make up 60 ml of formulations, as described in the Table 3. All the chemical formulations prepared were stirred at 25 ^oC for 12 h using a magnetic stirrer (IKA C-MAG HS 7 S002) set at 600 rpm. Thereafter, the formulations were sonicated at 25 Hz in an ultrasonic bath (Ultrasonics Corporation, USA) for 1 h to minimize particles agglomeration. They were then kept at 25 ^oC for aging.

2.3. Compatibility and stability study

Approximately, 60 ml of SiO_2-IBS formulations as shown in Fig. 1 were visually observed for 24 h at 25 and 100 ^oC, respectively, to find out the compatibility between the SiO_2 and IBS. The compatibility codes of A: homogenous solutions and B: precipitates were used to assess the compatibility studies. Furthermore, Fourier Transform Infrared Spectroscopy (FTIR) was conducted to establish the chemical interactions between the hybrid components as evidence of compatibility. For stability studies, four different experiments which include; pH control, viscosity enhancement, ultrasonication and particle size were conducted as described in (Ghadimi et al., 2011). After the normal pH of the solutions were recorded, the pH were then adjusted to 4, 6, 8, 10 and 12 using 1 N HCl and KOH, respectively, and visually observed at an interval of

time. Other fresh samples were prepared for stability test by viscosity enhancer method. Here a water soluble polymer, polyacrylamide (PAM) was used to increase the viscosity of base fluids in order to decrease the particle's speed to improve the stability. The concentrations of PAM used were 0.05, 0.1 and 0.15 % in the hybrid, while the controls (hybrid without PAM and SiO_2 with 0.05 % PAM) were also prepared. These were then visually observed for some time. In the ultrasonication test, two steps of sonication had been employed; firstly, the dispersion of SiO_2 in brine after 1 h of magnetic stirring was then sonicated in ultrasonic bath for 1 h. Thereafter, it was combined with the IBS and stirred for another 12 h. The solution was then sonicated for another 1 h and allowed to stand undisturbed and sedimentation rate was studied. In the last measurements, the particle size was determined using particle size analyzer (DT 1202). The SiO_2-IBS samples were placed in the measuring chamber equipped with a detector sensor to measure the particle's Brownian motions at 25 °C, from which the size was recorded.

2.4. Foamability screening study

Approximately, 10 ml of each sample including the pure IBS (control) was transferred into the Pyrex test tube as shown in Fig. 2. The solutions were mechanical shaken for 30 s to observe the relative foamability capacity. The maximum foam height was recorded in mm.

2.5. Thermal stability screening study

Viscosity retention capacity is used to evaluate the thermal stability of the chemical formulations. The dynamic viscosity of SiO_2-IBS hybrids and IBS solution were performed according to ASTM D445 using modular compact rheometer (MCQ 300). The viscosity was analyzed at 25 and 100 °C, and viscosity retention (thermal stability) capacity was computed according to Eq. 1.

$$Thermal\ stability = 100 - \left[\left(\frac{viscosty\ at\ 25℃ - viscosty\ at\ 100℃}{viscosty\ at\ 25℃}\right) \times 100\right] \quad (1)$$

2.6. Statistical analysis, modeling and optimization study

Analysis of variance (ANOVA) was used to statistically analyze the data obtained. The maximum criteria for foamability and viscosity retention (thermal stability) were set as a goal to obtain an optimum condition. The highest order polynomial with the significant terms was considered by taking cognizance of the model that is not aliased.

2.7. Particle partitioning at the foam lamella

Exactly 50 ml of the optimized SiO_2-IBS was placed in the graduated cylinder and vigorously shaken for 1 min to generate maximum foam volume. After 30 min, the liquid drainage was carefully poured out from the cylinder and the volume was recorded. The refractive index calibration curve of SiO_2 was generated (Fig. 3) to find the concentration (m/v %) of particles in the liquid drainage. This concentration was used to obtain the mass (g) of particles in the liquid drainage.

Fig. 1: The 20 different SiO_2-IBS formulations

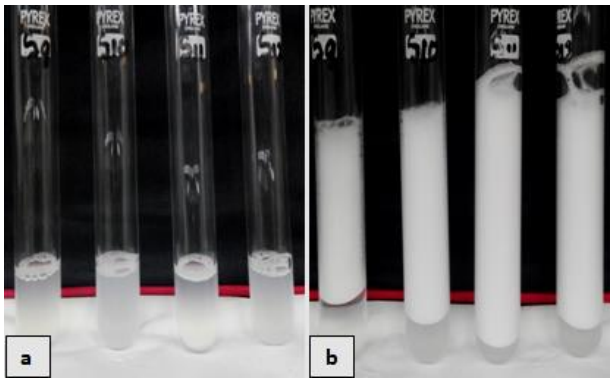

Fig. 2: Preliminary foamability test before foaming (a) and after foaming (b)

The percent mass of particle partitioning at the foam lamella was calculated according to the Eq. 2:

$$Percent\ mass = \frac{w_i - w_f}{w_i} \times 100 \quad (2)$$

Where, wi is the initial particles mass in the solution before foaming and wf is the particles mass in the liquid drainage after foaming.

2.8. Interfacial tension (IFT) measurement

The IFTs in oil/brine, oil/SiO_2 and oil/SiO_2-IBS systems were measured using Interfacial Tension Analyser (IFT 700) via a pendant drop. The oil droplets as shown in Fig. 4 were stabilized in the continuous phase for 1 min, and images were captured using a high resolution camera (Newport M-RS65). The IFT was analyzed by the DROPimange software according to Young-laplace equation by fitting the oil drop profile with the continuous phase (solution). Thereafter, the average IFT values were recorded.

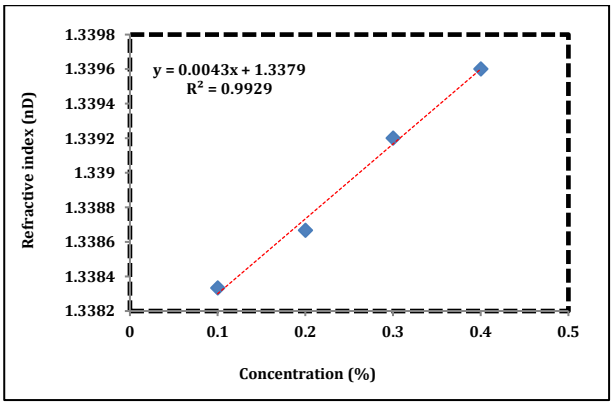

Fig. 3: Calibration curve of SiO_2

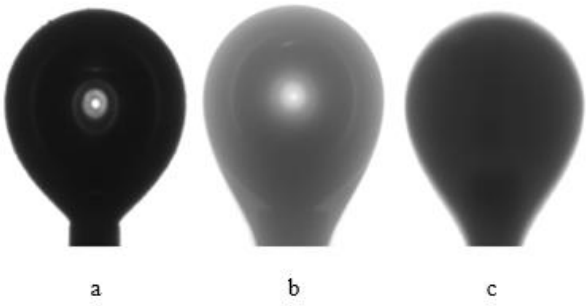

Fig. 4: Oil droplet in continuous phase of (a) brine (b) SiO_2 (c) SiO_2-IBS for IFT measurement

2.9. X-Ray diffraction (XRD) and field emission scanning electron micrograph (FESEM) characterizations

The XRD was recorded using Bruker D2 Phaser, while the surface morphology and texture was conducted using the FESEM instrument (Carl Zeiss AG SUPRA 55VP). The sample was coated with gold to minimize charges due to SiO_2 for proper viewing at different magnification from 100-100,000X.

3. Results and discussion

3.1. Result of compatibility and stability study

Compatibility study is commonly assessed by the formation of precipitates (Han et al., 2013). Precipitates occur due to lack of chemical interaction as a result of repulsive force. The SiO2 used in this study demonstrated good compatibility with IBS, because no precipitates were formed in all the SiO2-IBS hybrids formulated. The compatibility was further supported by FTIR experiments; the result is presented in Fig. 5. In the figure, the IFTR spectra of the pure dried SiO2 and SiO2-IBS hybrid were phased for easy comparison. The peaks absorbed at 1085.11 (sharped), 796.8, 563.8 cm-1 in the FTIR of the dried SiO2 were due to the Si-O-Si stretching, bending and rocking vibrations, respectively, which are also in accordance to findings in (Moore et al., 2003; Ryu and Tomozawa, 2006). Similarly, the FTIR spectrum of SiO2-IBS revealed the presence of a broad peak at 3319.52 cm^{-1} and additional peak at 1633.71 cm^{-1} due to the presence of N-H and C=O in the IBS. It can also be seen that the peak at 796.8 cm^{-1} in SiO_2 disappeared, and a bathochromic shift (redshift) was observed from 563.8 to 595.14 cm^{-1} revealing the formation of Si-C bond between the hybrid components. Similar observations were reported in SiO_2-polymer hybrid from the work of Zhu et al. (2014). In addition, a sharp intensity reduction of a SiO_2 peak at 1085.11 cm^{-1} was noticed in the SiO_2-IBS which further supported the chemical interaction between the SiO_2 an d IBS.

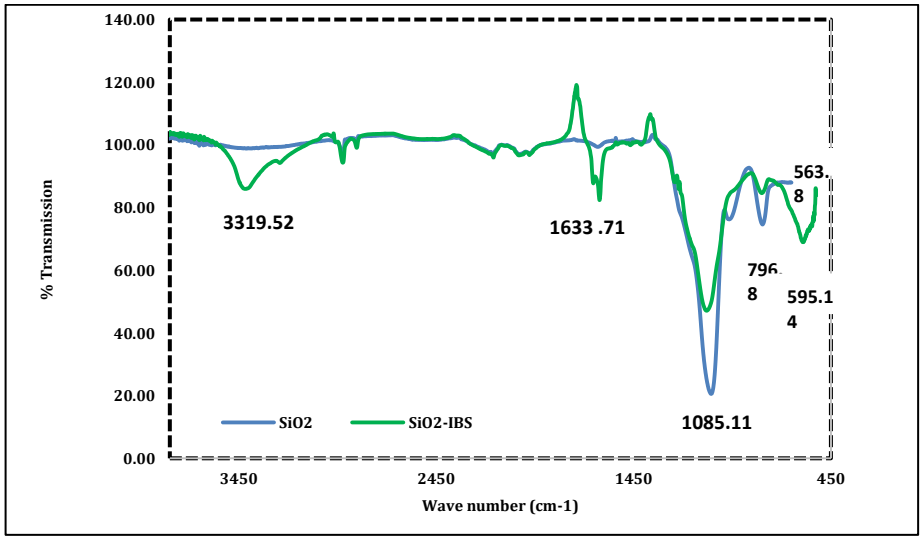

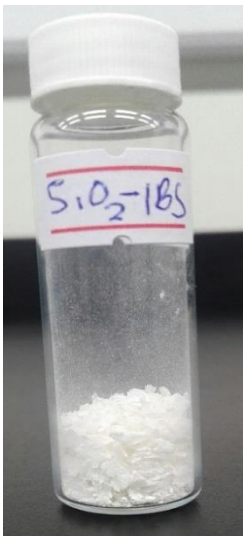

Fig. 5: FTIR spectra of pure SiO_2 and SiO_2-IBS hybrid

However, the stability of SiO_2-IBS was carefully studied by a visual test without any pH adjustment at 25 °C. The SiO_2-IBS had stability up to 8 h compared to the 3 h stability of pure SiO_2 dispersed in brine. To improve the stability of the dispersion, additional experiments were performed as described in (Ghadimi et al., 2011). pH control, viscosity enhancement and ultrasonication were selected for further stability test. In the pH control test, the normal pH of the dispersion at 25 °C was recorded to be 6.92. After the pH was adjusted to 4 8, 10 and 12, drastic and rapid precipitation of the dispersions

were observed in basic medium which typically indicated the destabilization of chemical interaction between the SiO_2 and IBS. While at pH 4 no precipitation was seen, but the dispersion had stability within 12 h. This finding is contrary to the report in (Ghadimi et al., 2015), where the authors claimed pH 10 as the optimized stability condition for nanofluid hybrid. Ghadimi et al. (2011) had explained the concept of Stoke's law in the field of nanofluid dispersions that by increasing the viscosity of base fluids would help to decrease particles speed and improve dispersion stability. Therefore, a water soluble polyacrylamide polymer (PAM) was incorporated in the SiO_2-IBS hybrid mixture at concentrations of 0.05, 0.1 and 0.15 % as shown in Fig. 6. The SiO_2-PAM without IBS was also prepared as a control. The same concentrations of SiO_2 and IBS were maintained in all the mixture. It was found out that addition of PAM in the SiO_2-IBS blend did not improve the stability, rather, the particles started to sediment immediately within 1 h and nearly sedimented at 6 h (Fig. 6b). No further changes were noticed up to 44 h of visual observations. This happened because some polymers caused particles to floc, which make them acquire higher density than the base fluid, and easily be dragged by gravity force (Derksen, 2014). In comparing with the SiO2-PAM blend, PAM had significant stabilization effect at a concentration of 0.05 %. Similar observation of the particle stabilization with PAM was reported in the work of Sharma et al. (2016), where the authors found that, SiO_2 blend containing surfactant and PAM induced additional flocculation of particles, which resulted to rapid particles sedimentation. Thus, PAM in our study could only improve the viscosity of SiO_2-IBS, but not its stability. However, in the ultrasonication experiment, it can be seen from the same figure that SiO_2-IBS (OPT) had been found to be stable up to 36 h with fewer particles still remained suspended after 48 h. In addition, Fig. 7 describe the rate of particles sedimentation as a function of time, it can be observed that SiO_2 in brine sediment faster than the SiO_2-IBS (OPT) hybrid, this is due to the electrical and sound vibration from the ultrasonic bath which broke down particle aggregations in the IBS and rendered them suspended in the medium (Mahbubul et al., 2017). To further support the ultrasonication stability, particle's size was measured. The particle size result is presented in Fig. 8. It can be seen from the figure that the particles are within the normal distribution and the agglomeration will not cause further destabilization (Chang et al., 2007).

3.2. X-Ray diffraction (XRD) result

The XRD result of pure dried SiO_2 is presented in Fig. 9a, from the figure it can be seen that SiO_2 exhibited characteristic of an amorphous nature due to the appearance of one broad diffraction shoulder between 20-30° at *2 theta*, which is typically the characteristic of amorphous silica. However, there was a slight transformation of nature from amorphous to crystalline like nature due the appearance of crystalline peaks as indicated in the XRD spectra of the hybrid material (Fig. 9b). This transformation was due to the interaction of SiO_2 and IBS.

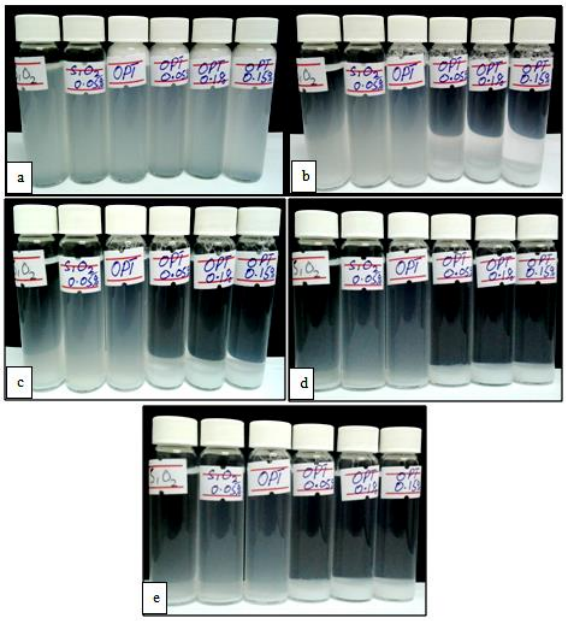

Fig. 6: Particles stabilization by ultrasonic bath after (a) 0 h, (b) 10 h, (c) 20 h, (d) 32 h and (e) 44 h

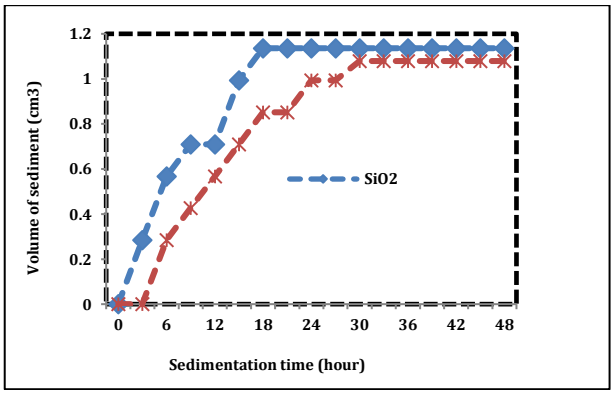

Fig. 7: Sedimentation rate of optimized hybrid surfactant (SiO_2-IBS) in comparison with SiO_2

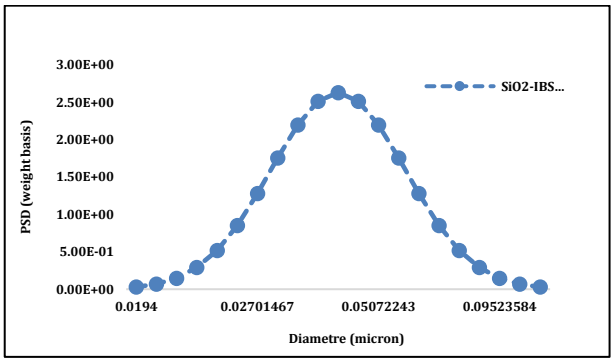

Fig. 8: Particle size distributions in nanofluid hybrid

3.3. Field emission scanning electron micrograph (FESEM) result

Fig. 10 is a field emission scanning micrograph (FESEM) of pure dried SiO_2 nanoparticle and SiO_2-IBS hybrid. From the Fig. 10a and 10b, it can be seen

that SiO_2 shows the morphology of network texture with pores. However, from the Fig. 10c and d of SiO_2-IBS, the surface network structure morphology of SiO_2 transformed to fine texture like and the pores were not seen, these indicated that IBS has been embedded within the structure.

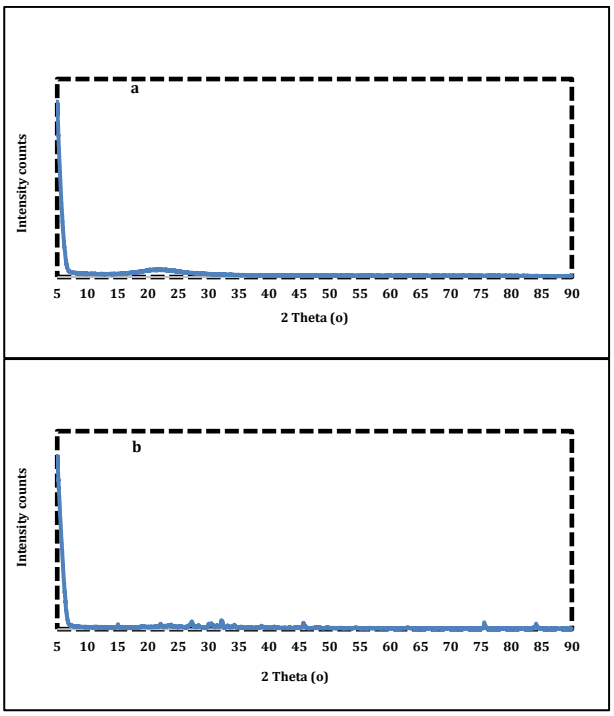

Fig. 9: XRD spectra of (a) pure dried SiO_2 (b) SiO_2-IBS hybrid

3.4. IFT result

The IFT for oil/brine system was found to be 120.3 ± 9.8 mN/m, this represented the existing interfacial force between the oil and brine. The dispersion of SiO_2 in the brine significantly lowered the IFT to 31.6 ± 3.9 mN/m. This is because SiO_2 has the ability to orient its hydrophilic and hydrophobic like parts in the aqueous and oil phase, respectively, and induced interfacial effect (Li et al., 2013). The SiO2-IBS blend had additional IFT reduction effect, and the result was found to be 10.6 ± 6.8 mN/m. This further reduction was a result of IBS surfactant in the blend, because surfactant is known as IFT reduction agents (Djemiat et al., 2015).

3.5. Result of foamability

The foamability data obtained were statistically analyzed and presented in Table 4. From the table, the value of prob. > F was found to be less than 0.05, indicating that the model terms (SiO_2, IBS, SiO_2*IBS, SiO_2^2 and aging) are significant. Similarly, the F value of 11.70 described the significance of the model chosen (cubic model). The R square value is used to evaluate the fitness of the model, so long it approaches unity (1.00) (Nguyen et al., 2014; Adamu et al., 2017). It can be seen that the R square of 0.8068 revealed that the model fits with the real data and this is confirmed by observing the small difference between the predicted (0.7379) and adjusted (0.5121) R square values.

Table 4: Analysis of variance (ANOVA) for foamability

Model	Sum of squares	Degree of freedom	Mean square	R square	Adjusted R square	Predicted R square	Adequate precision	F value	P value Prob. > F	
Model	3092.59	5.0	618.52	0.8068	0.7379	0.5121	12.767	11.70	0.0001	*significant*
A	392.64	1.0	392.64					7.42	0.0164	
AB	760.50	1.0	760.50					14.38	0.0020	
B^2	266.04	1.0	266.04					5.03	0.0416	
C	1452.92	1.0	1452.92					27.47	0.0001	
ABC	220.50	1.0	220.50					4.17	0.0605	
Residual	740.36	14.0	52.88							
Lack of fit	569.52	9.0	63.28					1.85	0.2575	*not significant*

A = [IBS], B = [SiO2] and C = Aging

The plot of residual data is shown in Fig. 11, the data can be seen to appear within the normal probability, and this further confirmed the fitness of the data obtained with the lack of fit value that is not significant. The adequate precision, which describe signal to noise ratio was found to be 12.767, and this is greater than 4 indicating the adequate signal precision. The cubic model developed is presented in Eq. 4, this describes a quantitative relationship between the foamability and the synergistic effects of the model terms (SiO_2, IBS SiO_2*IBS, SiO_2^2 and aging). Cubic model Eq. 3;

$$Foamability = +89.54 + 5.36*[IBS] - 9.75[IBS]*[SiO_2] + 4.26[SiO_2]^2 + 10.31[Aging] + 5.25\ [IBS]*[SiO_2]*[Aging] \quad (3)$$

Similarly, Fig. 12 shows the graphical interactions in three dimensional plots. From the graphs, it can be seen that the synergistic interaction of SiO_2 with IBS and aging showed that as the concentration of SiO_2 and IBS increases, the relative formability of SiO_2-IBS hybrid also increases. This indicates the surface activity of SiO_2 as a result of interaction with IBS which resulted to the increase in the relative foamability of the hybrid. Vatanparast et al. (2017) also observed similar phenomenon when they studied the synergistic interaction between SiO2 and SDS surfactant. Similarly, Mo et al. (2012) established that the foam height is directly proportional to the SiO_2 concentrations.

3.6. Result of particle partitioning at the foam lamella

The result of particle partitioning at the foam lamella demonstrated that foam generated in 1 min could result to 44 % of particles to be partitioned at

the foam lamella. This indicates that the SiO_2 has greater effect to be adsorbed at the foam lamella and stabilize the foam.

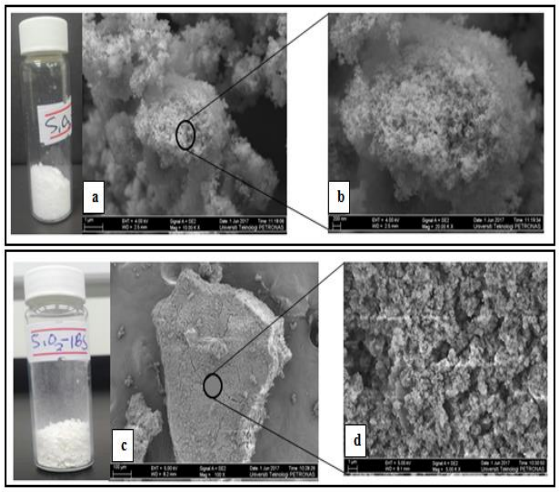

Fig. 10: FESEM micrograph of pure SiO_2 (a and b) and SiO_2-IBS hybrid (c and d)

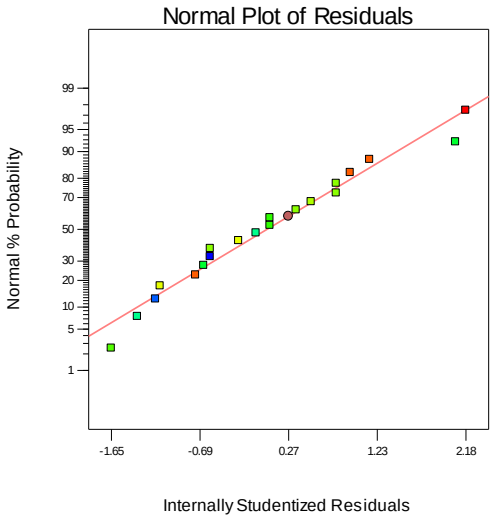

Fig. 11: Normal residuals plot of foamability data

3.7. Result of thermal stability

Thermal stability data obtained were also statistically analyzed similar to foamability. The ANOVA result is presented in Table 5. The model (cubic) and the model terms (SiO_2*IBS, IBS^2, aging, SiO_2*IBS*aging) are all significant.

The data were well fitted in the model and within the normal probability (Fig. 13). The synergistic effects between the model terms with respect to thermal stability were established in the developed model (Eq. 5). Fig. 14a shows that at relatively higher concentrations (#1.00) of IBS and SiO_2, the SiO_2-IBS hybrid had a maximum thermal stability at 100 ^oC. However, with respect to aging, the result shows that the hybrid is more stable at the early days (6 days). This indicates that aging is a crucial input parameter on the stability of hybrid. Cubic model Eq. 4:

$$Thermal\ stability = +15.74 + 4.56[IBS]^2 + 6.63\ [IBS]*[SiO_2] - 5.12[Aging] - 3.38\ [IBS]*[SiO_2]*[Aging] \quad (4)$$

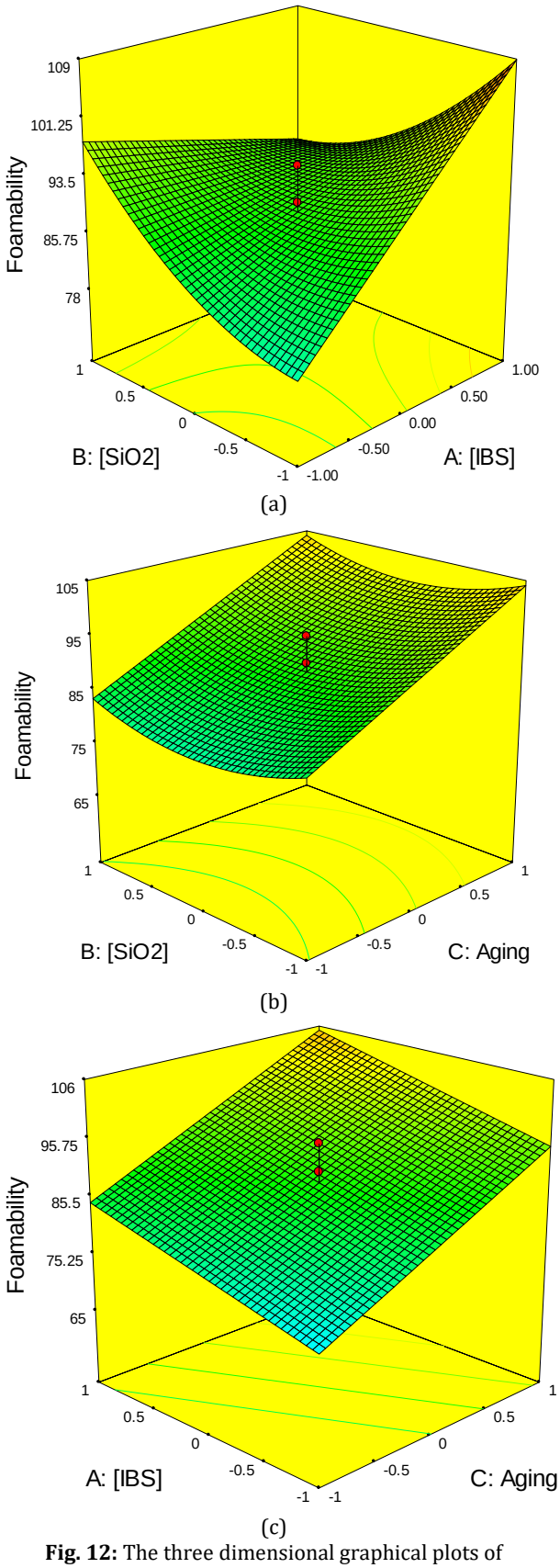

Fig. 12: The three dimensional graphical plots of foamability showing the synergistic interaction of SiO_2 with IBS (a), IBS with aging (b) and SiO_2 with aging (c)

3.8. Optimization and point prediction

After the establishment of the responses (foamability and thermal stability), the optimum condition could be achieved. The concentrations of SiO_2 and IBS and the aging time were kept within the range taken (-1.68 to +1.68), while the maximum value for foamability and thermal stability were set as criteria goals. Out of 18 optimum conditions generated, Table 5 shows the selected optimum condition based on the desirability which describes the extent to which goal criteria chosen to achieve the optimal conditions (Fig. 15).

To evaluate the accuracy of the developed models, an experiment was further conducted using the optimized conditions, and the result is presented in Table 6. From the table, the experimental values obtained for foamability and thermal stability were in good agreement with the values obtained from the predicted models. The minimum error observed indicates the accuracy of the cubic model for the foamability and thermal stability, respectively.

Table 5: Analysis of variance (ANOVA) for thermal stability

Model	Sum of squares	Degree of freedom	Mean square	R square	Adjusted R square	Predicted R square	Adequate precision	F value	P value Prob. > F	
Model	1105.38	4	276.35	0.7781	0.7190	0.5014	12.343	13.15	0.0001	*significant*
A^2	305.27	1	305.27					14.53	0.0017	
AB	351.13	1	351.13					16.71	0.0010	
C	357.86	1	357.86					17.03	0.0009	
ABC	91.13	1	91.13					4.34	0.0548	
Residual	315.17	15	21.01							
Lack of fit	281.67	10	28.17					4.20	0.0632	*not significant*

A = [IBS], B = [SiO2] and C = Aging

Table 6: Optimized conditions of SiO_2-IBS hybrid

Input variables (coded values)			Desirability	Predicted values		Experimental values		Error (%)	
IBS %	SiO2 %	Aging (days)		Foamability (mm)	Thermal stability (%)	Foamability (mm)	Thermal stability (%)		
1.0	1.0	1.0	0.681	96.4	23.1	100	25.4	3.6	9.1

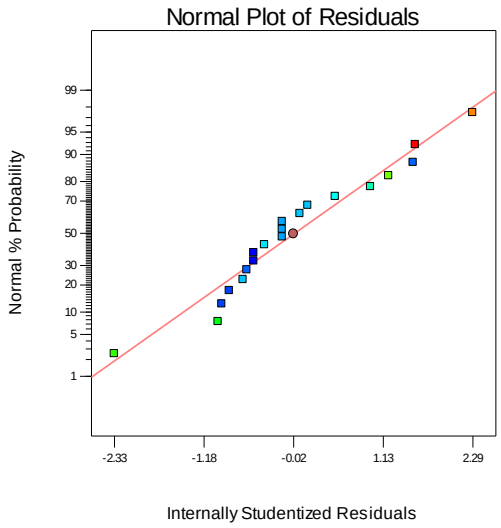

Fig. 13: Normal residual plot of thermal stability data

4. Conclusion

The following conclusions can be deduced from this study:

- A new EOR hybrid formulation (SiO_2-IBS) had been successfully developed, optimized and characterized.
- The effect of SiO_2 nanoparticles in the hybrid had been established to improve the relative foamability, thermal stability and IFT reduction between crude oil and brine
- Two multivariate models (cubic) were developed and validated, and the synergistic interaction between the components were quantified.
- This novel hybrid material could find wide applications in the EOR, particularly, in the higher temperature reservoirs.

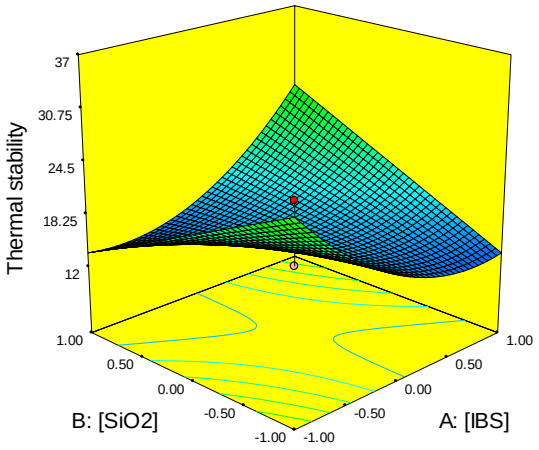

(a)

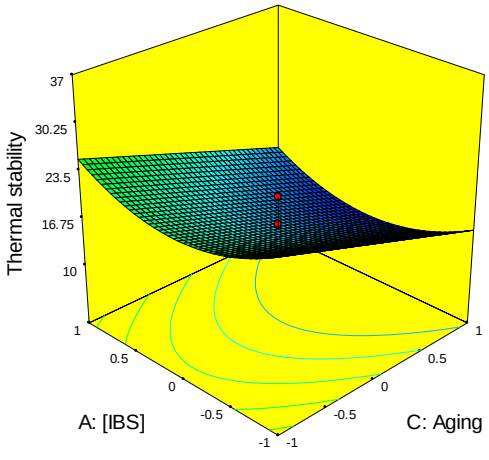

(b)

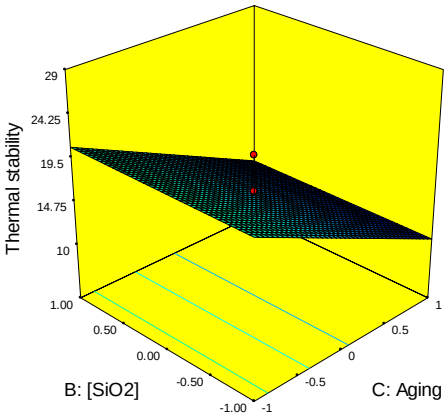

(c)

Fig. 14: The three dimensional graphical plots of thermal stability showing the synergistic interaction of SiO_2 with IBS (a), SiO_2 with aging (b) and IBS with aging (c)

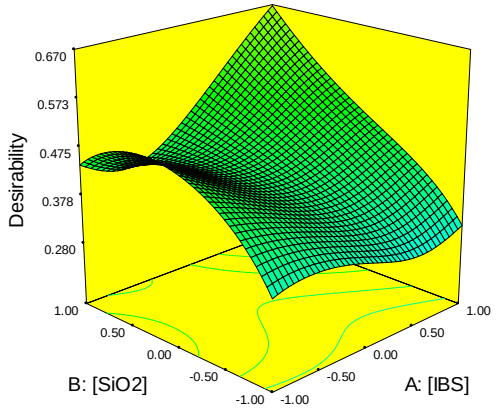

Fig. 15: Desirability response for optimum condition

Acknowledgement

The authors would like to express their sincere and honest gratitude to the Enhance Oil Recovery Mission Oriented Research Group of Universiti Teknologi PETRONAS, and Exploration, Production and Technical Department of PETRONAS, Malaysia for studentship support and financing the project (Grant No. EPTD T1.3), respectively.

References

Adamu M, Bashar SM, and Shafiq N (2017). Flexural performance of nano silica modified roller compacted rubbercrete. International Journal of Advanced and Applied Sciences, 4(9): 6-18.

Ahmadi Y, Eshraghi SE, Bahrami P, Hasanbeygi M, Kazemzadeh Y, and Vahedian A (2015). Comprehensive Water–Alternating-Gas (WAG) injection study to evaluate the most effective method based on heavy oil recovery and asphaltene precipitation tests. Journal of Petroleum Science and Engineering, 133: 123-129.

Alagorni AH, Yaacob ZB, and Nour AH (2015). An overview of oil production stages: enhanced oil recovery techniques and nitrogen injection. International Journal of Environmental Science and Development, 6(9), 693-701.

Chang H, Joo SH, and Pak C (2007). Synthesis and characterization of mesoporous carbon for fuel cell applications. Journal of Materials Chemistry, 17(30): 3078-3088.

Derksen J (2014). Simulations of hindered settling of flocculating spherical particles. International Journal of Multiphase Flow, 58: 127-138.

Djemiat DE, Safri A, Benmounah A, and Safi B (2015). Rheological behavior of an Algerian crude oil containing Sodium Dodecyl Benzene Sulfonate (SDBS) as a surfactant: Flow test and study in dynamic mode. Journal of Petroleum Science and Engineering, 133: 184-191.

Esmaeeli Azadgoleh J, Kharrat R, Barati N, and Sobhani A (2014). Stability of silica nanoparticle dispersion in brine solution: an experimental study. Iranian Journal of Oil and Gas Science and Technology, 3(4): 26-40.

Ghadimi A, Metselaar HSC, and Lotfizadehdehkordi B (2015). Nanofluid stability optmization based on UV-vis spectrophotometer measurement. Journal of Engineering Science and Technology, 10: 32-40.

Ghadimi A, Saidur R, and Metselaar HSC (2011). A review of nanofluid stability properties and characterization in stationary conditions. International Journal of Heat and Mass Transfer, 54(17): 4051-4068.

Hamza MF, Sinnathambi CM, and Merican ZMA (2017). Recent advancement of hybrid materials used in chemical enhanced oil recovery (CEOR): A review. In the 29th Symposium of Malaysian Chemical Engineers: Materials Science and Engineering Conference Series, Miri, Sarawak, Malaysia, 206(1): 1-9. https://doi.org/10.1088/1757-899X/206/1/012007

Han M, Alsofi A, Fuseni A, Zhou X, and Hassan S (2013). Development of chemical EOR formulations for a high temperature and high salinity carbonate reservoir. In the International Petroleum Technology Conference, Beijing, China. http://doi.org/10.2523/17084-MS

Kapetas L, Bonnieu SV, Danelis S, Rossen W, Farajzadeh R, Eftekhari A, Shafian SM, and Bahrim RK (2016). Effect of temperature on foam flow in porous media. Journal of Industrial and Engineering Chemistry, 36: 229-237.

Li S, Hendraningrat L, and Torsaeter O (2013). Improved oil recovery by hydrophilic silica nanoparticles suspension: 2 phase flow experimental studies. In the International Petroleum Technology Conference, Beijing, China.

Mahbubul IM, Elcioglu EB, Saidu R, and Amalina MA (2017). Optimization of ultrasonication period for better dispersion and stability of TiO2–water nanofluid. Ultrasonics Sonochemistry, 37: 360-367.

Mo D, Yu J, Liu N, and Lee RL (2012). Study of the effect of different factors on nanoparticle-stablized CO2 foam for mobility control. In the SPE Annual Technical Conference and Exhibition, Society of Petroleum Engineers, San Antonio, Texas, USA. https://doi.org/10.2118/159282-MS

Moore C, Perova TS, Kennedy B, Berwick K, Shaganov II, and Moore RA (2003). Study of structure and quality of different silicon oxides using FTIR and Raman microscopy. In the Society of Photo-Optical Instrumentation Engineers (SPIE) Conference Series, Optics and Photonics Technologies and Applications, Galway, Ireland, 4876: 1247-1256. https://doi.org/10.1117/12.464024

Muggeridge A, Cockin A, Webb K, Frampton H, Collins I, Moulds T, and Salino P (2014). Recovery rates, enhanced oil recovery and technological limits. Philosophical Transactions (Series A): Mathematical, Physical, and Engineering Sciences, 372: 1-25.

Nguyen XH, Bae W, Gunadi T, and Park Y (2014). Using response surface design for optimizing operating conditions in recovering heavy oil process, Peace River oil sands. Journal of Petroleum Science and Engineering, 117: 37-45.

Qureshi Z, Ashqar A, Banyopadhyay I, and Al hammadi K (2016). Successful flood-front and breakthrough prediction of miscible wag in a complex carbonate reservoir-a case study. In the Abu Dhabi International Petroleum Exhibition and

Conference. Society of Petroleum Engineers, Abu Dhabi, UAE. https://doi.org/10.2118/183362-MS

Riazi M and Golkari A (2016). The influence of spreading coefficient on carbonated water alternating gas injection in a heavy crude oil. Fuel, 178: 1-9.

Ryu SR and Tomozawa M (2006). Fictive temperature measurement of amorphous SiO 2 films by IR method. Journal of Non-Crystalline Solids, 352(36): 3929-3935.

Shabib-Asl A, Ayoub M, Alta'ee A, Saaid IBM, and Valentim PPJ (2014). Comprehensive review of foam application during foam assisted water alternating gas (FAWAG) method. Research Journal of Applied Sciences, Engineering and Technology, 8(17): 1896-1904.

Sharma T, Iglauer S, and Sangwai JS (2016). Silica nanofluids in an oilfield polymer polyacrylamide: Interfacial properties, wettability alteration, and applications for chemical enhanced oil recovery. Industrial and Engineering Chemistry Research, 55(48): 12387-12397.

Sun L, Pu W, Xin J, Wei P, Wang B, Li Y, and Yuan C (2015). High temperature and oil tolerance of surfactant foam/polymer–surfactant foam. RSC Advances, 5(30): 23410-23418.

Tunio SQ and Chandio TA (2012). Recovery enhancement with application of FAWAG for a Malaysian field. Journal of Applied Sciences, Engineering and Technology, 4: 8-10.

Vatanparast H, Samiee A, Bahramian A, and Javadi A (2017). Surface behavior of hydrophilic silica nanoparticle-SDS surfactant solutions: I. Effect of nanoparticle concentration on foamability and foam stability. Colloids and Surfaces A: Physicochemical and Engineering Aspects, 513: 430-441.

Xue Z, Worthen A, Qajar A, Robert I, Bryant SL, Huh C, Prodanović M, and Johnston KP (2016). Viscosity and stability of ultra-high internal phase CO 2-in-water foams stabilized with surfactants and nanoparticles with or without polyelectrolytes. Journal of Colloid and Interface Science, 461: 383-395.

Zhu D, Wei L, Wang B, and Feng Y (2014). Aqueous hybrids of silica nanoparticles and hydrophobically associating hydrolyzed polyacrylamide used for EOR in high-temperature and high-salinity reservoirs. Energies, 7(6): 3858-3871.